The direction of protein entry into the proteasome determines the variety of products and depends on the force needed to unfold its two termini

Published version:

DOI:10.1016/j.molcel.2012.08.029

The Direction of Protein Entry into the Proteasome Determines the Variety of Peptide Products and Depends on the Force Needed to Unfold Its Two Termini

Dikla Berko[1], Shira Tabachnick[1], Dalit Shental-Bechor[2], Paolo Cascio[3], Silvia Mioletti[3], Yaakov Levy[2], Arie Admon[4], Tamar Ziv[4], Boaz Tirosh[5], Alfred L. Goldberg[6] & Ami Navon[1*]

[1]Department of Biological Regulation, The Weizmann Institute of Science, Rehovot, 76100, Israel.
[2]Department of Structural Biology, The Weizmann Institute of Science, Rehovot, 76100, Israel.
[3]Department of Veterinary Morphophysiology, Turin University, v. L. da Vinci 44 - 10095 Grugliasco, Italy.
[4]Department of Biology, Technion - Israel Institute of Technology, Haifa, 32000, Israel.
[5]The Institute for Drug Research, The School of Pharmacy, The Hebrew University of Jerusalem, P.O. Box 12065, Jerusalem 91120, Israel.
[6]Department of Cell Biology, Harvard Medical School, 240 Longwood Ave. Boston MA 02115 USA.

[*]Correspondence should be addressed to:

e-mail: ami.navon@weizmann.ac.il

ABSTRACT

Poorly structured domains in proteins enhance their susceptibility to proteasomal degradation. To learn whether the presence of such a domain near either end of a protein determines its direction of entry into the proteasome, directional translocation was enforced on several proteasome substrates. Using archaeal PAN-20S complexes, mammalian 26S proteasomes and cultured cells, we identified proteins that are degraded exclusively from either the C or N terminus and some showing no directional preference. This property results from interactions of the substrate's termini with the regulatory ATPase and could be predicted based on the calculated relative stabilities of the N and C termini. Surprisingly, the direction of entry into the proteasome affected markedly the spectrum of peptides released and consequently influenced the efficiency of MHC class I presentation. Thus, easily unfolded termini are translocated first, and the direction of translocation influences the peptides generated and presented to the immune system.

INTRODUCTION

26S proteasomes are composed of two sub-complexes, the 19S regulatory particle and the 20S proteolytic component. The 20S core particle is a barrel-shaped hollow complex, made of four stacked heptameric rings, two outer α-rings and two inner β-rings ($\alpha_{1-7}\beta_{1-7}\beta_{1-7}\alpha_{1-7}$). Three of these β subunits harbor its proteolytic sites, which are found within the central chamber of the 20S complex sequestered from the bulk solution (Groll et al., 1997; Lowe et al., 1995a). Substrates enter the 20S particle through a gated channel in the α ring (Groll et al., 2000; Whitby et al., 2000). This gated narrow orifice (~15Å) allows the entry only of unfolded polypeptides. The gate is formed by the α-subunits' N-termini and is regulated by the associated 19S ATPase ring (Medalia et al., 2009; Rabl et al., 2008; Smith et al., 2005). Consequently, a globular substrate must undergo unfolding by the AAA ATPases of the 19S complex (Rpt1-6) prior to translocation and digestion. This process entails recognition and binding of the protein substrate to the 19S complex, generally via the conjugated ubiquitin chain.

Recent studies indicate that for efficient proteasomal degradation, in addition to the polyubiquitin tag, a substrate must contain a loosely folded or unfolded region that is engaged first with the proteasomal unfolding or translocation machinery, and in effect appears to serve as the degradation initiation site (Prakash et al., 2004; Shabek et al., 2009; Takeuchi et al., 2007). Globular proteins that lack an inherently loose domain fail to bind tightly to the 26S proteasome, even when polyubiquitinated and are inefficiently degraded (Peth et al., 2010). However, degradation is improved when an unstructured region is attached near their termini (Prakash et al., 2004; Takeuchi et al., 2007). While some proteins may harbor a loose domain(s) or termini, the association with the proteasome can also promote partial unraveling of a terminus (Hagai and Levy, 2010). Alternatively, p97/VCP complex may expose these domains and facilitates proteasomal degradation (Beskow et al., 2009).

So far, there have been no systematic studies of the direction of polypeptide degradation by proteasomes, and whether such directionality may reflect conformational properties of the substrate's termini or if the direction of entering the proteasome influences the nature of products generated. Here, we examined the influence of the substrate's terminal domains on the direction of translocation into the proteasome and on product generation. We show that while *in vitro* certain proteins are exclusively degraded from their N or C termini, others can be degraded from either end, and that inherent specific manner of directionality also occurs during proteasomal degradation *in vivo*. Directionality is conferred by the proteasome-regulatory ATPase complex, since the core 20S particle by itself did not possess any inherent directional preference for protein digestion. Most importantly, directionality can be predicted *in silico* based on calculations of the force needed to unravel the N versus the C terminal tails. In contrast to terminal entry, translocation into the proteasome from an internal loop can lead to the sparing from degradation of the neighboring globular domains. A mechanism that may account for the processing of certain transcription factors (e.g. NF-κB, MGA2 or SPT23) from their larger precursors (Hoppe et al., 2000).

Finally, our results demonstrate that the direction of polypeptide degradation influences the spectrum of peptides released by the proteasome. Furthermore, we directly demonstrate that the directionality of a polypeptide digestion by the proteasome modulates MHC Class I presentation of specific antigens, as these peptides serve as precursors for the antigenic peptides presented on the cell surface to the immune system.

RESULTS

Maltose Binding Protein (MBP) is degraded in a C to N direction

To test whether degradation of proteins by the archaeal PAN-proteasome complex and the mammalian 26S proteasome occurs from a preferred terminus, we linked several protein substrates through either end to a blocking moiety unable to translocate through the central pore in the ATPaes ring. Initially, we covalently linked Maltose Binding Protein (MBP) of *E. Coli* to a solid phase (agarose beads) by inserting a cysteine residue either at the N or C-terminus. In addition, a sequence encoding a 6-His tag was attached to the other terminus to facilitate isolation and analysis by Western blot. The two purified MBP variants were then linked covalently through the cysteines to iodoacetamido-agarose beads leaving either the C or N-terminus free. As shown in Figure 1A, blotting for His tag revealed that only MBP linked to the matrix through its N-terminus was degraded over time upon incubated with PAN, 20S proteasomes and ATP at 55°C. Blotting with an anti-MBP polyclonal antibody confirm that the MBP molecules were completely degraded, not just the region bearing the His-tag (not shown). Degradation required proteasomes, PAN, as well as ATP (supplementary Figure S1A). Thus, degradation of MBP by the PAN-20S complex occurs only from its C-terminus.

To check if this exclusive degradation from the C-terminus is an inherent property of MBP and not a consequence of attachment to the agarose, we linked MBP to streptavidin from either side. The cysteine residue was reacted with iodoacetamido-biotin and subsequently bound to streptavidin-coated PCR tubes, leaving the other terminus free (Navon and Goldberg, 2001). After washing unbound MBP, buffer containing ATP, PAN, and proteasomes was added, and the tubes were incubated at 55°C. As shown in supplementary Figure S1B, again only the MBP bound to the streptavidin through its N-terminus was degraded in PAN-and ATP-dependent manner corroborating the C to N directionality for MBP degradation.

β–casein is degraded exclusively in an N to C direction by PAN-20S and the 26S proteasomes

To test if the degradation of other proteins by the PAN-20S complex also occurs in a preferred direction, we examined β-casein, which is widely used as a substrate for proteasomes and ATP-dependent proteases. When agarose-bound casein derivatives (prepared in a similar fashion to that described for MBP) were incubated with PAN-20S and ATP, only the casein attached through its C-terminus was degraded (Figure 1B), as was confirmed by anti-His-tag and anti-biotin immunoblotting. Thus, casein is also degraded in a directional fashion, however from N to the C terminus, opposite to MBP degradation.

This conclusion was confirmed by biotinylating casein and attachment to avidin, which blocks translocation through the PAN ring (Navon and Goldberg, 2001) (supplementary Figure S1C). Thus, degradation of casein in solution is also contingent on a free N terminus. The results obtained for MBP and casein indicate that ATP-dependent translocation of substrates by PAN can occur from either end in a substrate specific manner.

To determine whether β-casein is also degraded in an N to C direction by mammalian 26S proteasomes, we compared the degradation of casein, biotinylated on either its N or C terminus, to its degradation when these biotin moieties were linked to an avidin moiety. β-casein was degraded by 26S proteasomes when it was biotinylated on either terminus or attached to avidin on its C-terminus. However, when the N-terminus of casein was bound to avidin, it resisted proteasomal degradation (Figure 1C). To exclude the possibility of partial degradation of the casein molecule, we used antibodies directed to both termini (i.e. anti His-tag and anti-biotin antibodies), which yielded similar conclusions. Thus, casein is degraded by mammalian 26S exclusively from its N-terminus, as was found with the archaeal PAN-20S complex. Control incubations without 26S or containing 26S and the specific proteasome inhibitor, bortezomib (Velcade), confirmed that degradation was catalyzed by the added proteasomes (supplementary Figure S1D). This directionality was surprising since casein is usually viewed as a loosely folded or unfolded molecule; however, it contains a hydrophobic C-terminus and a highly charged N-terminus (Swaisgood, 2003), and presumably these structural differences account for the exclusive N to C degradation.

20S proteasomes degrade casein from either terminus

This inability of the 26S particles to degrade casein from its C-terminus might be due to a failure of PAN and the 19S particle to recognize or translocate this region of casein or due to a selective property of the 20S proteolytic particle. To distinguish between these possibilities, we conducted degradation reactions in the presence of SDS-activated 20S proteasomes. When casein biotinylated on its C- or N-terminus was incubated with the activated 20S proteasomes, it was degraded rapidly in both configurations. The attachment of avidin to the N- or the C-terminal biotin did not prevent degradation (Figure 1D). Again, the complete hydrolysis of the casein was confirmed using antibodies against both the His-tag and biotin. Thus, the 20S proteasome by itself has no apparent preference for a specific terminus of casein indicating that the direction-specific degradation by the 26S and PAN-20S complex is governed by the 19S or PAN and thus presumably by the interaction of casein and the ATPases.

The degradation of apo-calmodulin proceeds from either terminus.

Unlike MBP or casein, calmodulin has a rather symmetrical tertiary structure, in which its N and C termini have similar architectures (Kuboniwa et al., 1995). If the directions of translocation found for MBP and casein, in fact, are determined by the properties of their N- or C-termini, then calmodulin should be degraded equally well from both termini. We thus fused RFP to calmodulin’s N-terminus (RFP-calmodulin) or to its C-terminus (calmodulin-RFP). When either of these fusion proteins was incubated with PAN-20S and ATP, the fluorescence of RFP did not decrease. Thus, the RFP portion of the fusion proteins was neither degraded nor unfolded. Western blot analysis with anti-RFP antibodies demonstrated that the calmodulin portion of the fusion proteins was largely digested, regardless of whether calmodulin was located upstream or downstream to the RFP domain (Figure 1E). Thus, although some partial degradation products of calmodulin were detected, especially when its C-terminus was blocked, the breakdown of apo-calmodulin (in contrast to casein and MBP) can start from either its N- or C-terminus.

Purified 26S and 20S proteasomes degrade p21 and denatured ovalbumin from either terminus

To define further the structural features that determine the direction of degradation, we analyzed the breakdown of two proteins with poorly defined structures, the cyclin-dependent kinase inhibitor, p21, and denatured ovalbumin (Ova). Previous work suggested that p21 binds to proteasomes directly, and its degradation occurs independently of ubiquitination (Chen et al., 2004). Purified p21 was fused through either of its termini to RFP, as described for calmodulin. The two fusion proteins, p21-RFP and RFP-p21 were incubated at 37ºC with purified 26S or 20S proteasomes in the absence of SDS. Blotting for RFP demonstrated that the p21 portion of both chimeric proteins was digested by both 20S and 26S proteasomes (Figure 2A & B respectively). Thus, like calmodulin, degradation of p21 readily proceeds from either terminus (although at different rates). The degradation was incomplete and generated a significant amount of RFP-containing polypeptide that was not proteolysed further (Figure 2C & supplementary Figure S2).

Native ovalbumin is digested poorly by both 20S and 26S proteasomes, but denatured ovalbumin is rapidly degraded by both (Kohler et al., 2001). We prepared two derivatives of ovalbumin lacking the N-terminal 51 residues signal peptide (Shen and Rock, 2004), fused through either terminus to RFP (termed Ova-RFP and RFP-Ova). To facilitate degradation, we denatured the purified proteins by guanidinium-HCl, followed by immediate desalting. These treatments confer a molten globule-type structure (Kohler et al., 2001; Tani et al., 1997). As shown in Figure 2D, both derivatives of ovalbumin were degraded by 26S proteasomes at different rates. Again, in both cases most of the RFP domains were spared (supplementary Figure S2C). These findings indicate that poorly structured proteins can be degraded by the proteasome from either end.

Proteins can be degraded in a preferred direction in living cells

Next, we tested whether directional degradation also occurs in living cells. The two RFP derivatives of p21 and ovalbumin were cloned into a retroviral expression vector and these constructs were used to transduce EL4 cells (mouse thymoma). To investigate the stability of the RFP-fused variants of p21 and ovalbumin *in vivo*, the cells were treated with cycloheximide to block protein synthesis, and degradation was assayed in the presence and absence of the proteasome inhibitor. The two variants of p21 attached to RFP either through the N or C terminus were degraded at roughly similar rates in a proteasome-dependent manner (Figure 3A & 4C). Thus, the degradation of p21 proceeded from either terminus *in vivo* as was found *in vitro* (Figure 2A & B).

In contrast, the two ovalbumin-containing chimeric proteins were degraded differently. While ovalbumin-RFP was efficiently eliminated by the proteasome with a half-life of about two hours, the N-terminal derivative, RFP-ovalbumin, remained stable and resisted degradation (Figure 3B). These results clearly indicate N→C degradation *in vivo*, and not surprisingly, differ from those obtained with the hydrolysis by purified proteasomes of the denatured (molten globule) form of ovalbumin (where both termini are loosely packed). These results imply that a protein's terminal regions can have a significant role in initiation of proteasomal degradation *in vivo* as they do *in vitro*.

Initiation of degradation in an internal unstructured region

One possible alternative explanation for the lack of directionality during degradation of the p21 fusions (and also during *in vitro* degradation of the ovalbumin and calmodulin fusions) is that these substrates are not translocated into the 20S from either terminus but instead from an internal region that enters the proteasome as a loop. Such a mechanism was first demonstrated *in vitro* (Liu et al., 2003) and is possible here since these proteins are believed to be loosely folded or unstructured (and thus capable of forming loops). To test this possibility, we constructed a p21 derivative with both ends blocked (6His-GFP-p21-CFP-Flag) and purified it from *E. coli*. As shown in Figure 4A, despite the blocks on both termini, the central p21 domain was degraded by the 26S proteasomes, while both the N-terminal (GFP) and the C-terminal (CFP) blocking domains were spared, as was shown by immunoblots of these domains (with the anti His and Flag antibodies).

To assess whether 6His-GFP-p21-CFP-Flag is processed in a similar manner in living cells, we expressed this construct in EL4 cells. As was found *in vitro*, both the GFP and the CFP domains resisted degradation and large amounts of each accumulated. CHX chase demonstrated that the connecting p21 sequence was completely digested by the proteasome, as evident from the stabilization of the full-length protein in the presence of bortezomib (Figure 4B). The accumulation of the GFP and CFP in EL4 cells was in sharp contrast to their processive degradation when only one terminus of p21 was blocked (i.e. in RFP-p21 & p21-RFP) (Figure 4C). The released protecting CFP and GFP domains were very stable (half-lives >12h, data not shown) and thus were much more abundant than the full-length proteins (whose initial levels reflected only the molecules protected from degradation by bortezomib treatment). Thus, both *in vitro* and in cells, 26S proteasomes can translocate and degrade multidomain proteins beginning at an unstructured internal domain, but do so in a nonprocessive manner. This degradation from an internal loop in the case of p21 and ovalbumin (see below) had very different consequences (i.e. distinct products); therefore, the processive directional degradation of substrates with a single blocked terminus described above (both *in vitro* and *in vivo*) is a distinct process and can not be due to initiation from an internal loop within the loosely folded domains. Conversely, it is very unlikely that the degradation of the doubly blocked substrates in cells is due to an internal cleavage by cellular protease, followed by proteasomal digestion from the exposed free end.

The direction of substrate translocation affects the spectrum of peptide products generated

Proteasomes generate the antigenic peptides presented to the immune system on surface MHC Class I molecules (Rock and Goldberg, 1999; Rock et al., 2002). The two modes of polypeptide entry into the proteasome might influence the peptide products generated and thus the repertoire for antigen presentation. To test this we analyzed by mass spectrometry the degradation products from the two RFP derivatives of p21 and ovalbumin. It should be noted that our mass spectrometry analysis is suitable to detect peptides longer 6 residues, which comprise the majority of proteasome products (Kisselev et al., 1999; Kohler et al., 2001). Consequently, this analysis focuses on peptides longer than 7 residues, which correspond to the lengths that are eventually utilized for antigen presentation.

Initially, we analyzed the products generated upon degradation of denatured (molten globule) ovalbumin by the mammalian 20S proteasome, which do not exhibit a directional preference. A total of 116 peptides were detected from ovalbumin-RFP and 119 from RFP-ovalbumin. Of these, 78 (about 66%) peptides were found in both preparations (common), and the rest (about 34%) were found only upon degradation from one direction (Table S1, Figure S3A). A similar analysis was performed after incubation of the two p21 derivatives with either the 20S or 26S proteasomes. As shown in Table S1 & Figures S3B & C, about 40-50% of the peptide products were generated from p21 with either its C- or N-terminus blocked. The remaining 50-60% of the products was detected only upon degradation from a specific terminus. Thus, large differences in the spectrum of peptides produced by either 20S or 26S are seen when a substrate is degraded from its C- or N-terminus. Importantly, the peptides that were generated in a direction-specific fashion were derived from all regions of the substrate.

The direction of translocation strongly affects the diversity and abundance of peptide products

Because this type of MS analysis does not provide quantitative information about peptide abundance and does not allow comparisons of the relative amounts of these products, we also measure the relative amounts of identical and unique peptides generated from RFP-p21 and p21-RFP during digestion by 26S proteasomes. Derivatizing the degradation products with fluorescamine indicated that in total about five times more peptides were generated during digestion of p21-RFP than when RFP-p21 was degraded.

Based on this analysis, we prepared a mixture containing equal amounts of peptide products from the degradation of each substrate. One of the samples was derivatized by reductive dimethylation with deuterium-and ^{13}C, 'heavy', formaldehyde and the other treated with non-isotopic formaldehyde. The samples were mixed, and the isotopic ratios in the individual peptides analyzed. As shown in Figure 5A & S4A, the efficiency with which some of the peptides were generated was dramatically different upon degradation from the opposite termini, in agreement with the findings presented in Figure S3 & Table S1. Of the 135 peptides identified, about 40% were generated at equal efficiency whichever terminus of p21 entered the proteasome first. About 60% of the peptides recovered were at least two fold or in many cases much more abundant when p21 was degraded from either direction. Similar analyses were also carried out with the samples labeled with heavy isotopes or formaldehyde in the reciprocal fashion and gave similar results (Figure S4B). In all of these reactions, substrates were present in large excess, and not more than a third of the initial substrate was consumed (supplementary

Figure S5). Therefore, it is most likely that the peptides analyzed were generated directly from the protein substrate (while degradation was linear) and did not reenter the proteasome for successive rounds of proteolysis.

The differences in the diversity of peptide products could have been explained if the products generated by the proteasome were affected by the direction or rate of translocation. To test this possibility we analyzed the products size distribution of by gel filtration (Kisselev et al., 1998). The peptides generated from both p21-RFP and RFP-p21 by 26S proteasomes had a continuum of sizes, ranging from 2-27 residues (Figure 5B). The mean length (5.9 residues) and median length (3.9 residues) (supplemental Table S2) and the size distributions of peptides (Figure 5B) were indistinguishable when degradation proceeded C to N or N to C, and both fit a log-normal distribution, in accord with previous analysis of different substrates and proteasome species (Cascio et al., 2002; Cascio et al., 2001; Kisselev et al., 1998; Kisselev et al., 1999; Kohler et al., 2001). Thus, the frequency of polypeptide cleavages per protein and hence mean size of the products was not influenced by the direction of translocation into the proteasome, even though the efficiency of generating different peptides was very different.

The direction of translocation determines the efficiency of presentation of an MHC class I epitope.

These findings with isolated proteasomes predict that *in vivo* the direction of substrate entry into the proteasome should modulate presentation on MHC class I molecules. To directly test this, we compared the presentation of the immunodominant epitope from ovalbumin, SIINFEKL, in EL4 cells expressing the two versions of ovalbumin that are digested in distinct manners: HA-RFP-ova-RFP-His which can only be translocated into the proteasome from the internal ovalbumin domain (Figure 6A), and ova-

RFP-His which can only be digested from its N-terminus, (Figure 3). EL4 cells expressing HA-RFP-ova-RFP-His or ova-RFP-His were analyzed by flow cytometry for the levels of H-2K^b/SIINFEKL complexes by staining with 25-D1.16, a monoclonal antibody specific for this complex (Porgador et al., 1997). H-2K^b/SIINFEKL complexes were hardly detected in the cells expressing RFP-ova-RFP but were clearly evident in the cells expressing ova-RFP (1/1000) (Figure 6B). This difference demonstrates that the mode of ovalbumin entry into the proteasome (through an internal loop versus a terminal region) markedly affects the amount of this epitope presented on MHC class I complexes, as predicted by our studies with isolated proteasomes and pure substrates.

In these experiments the level of H-2K^b/SIINFEKL complexes was monitored at steady state conditions; however, the H-2K^b/SIINFEKL complex is quite stable, with a half life of about 6 hours (Howarth et al., 2004), suggesting that on a shorter time scale or for less stable MHC class I-peptides complexes, the effect would be even more dramatic. These findings on a single easily quantitated epitope further distinguish degradation from an internal domain and a loosely folded terminus and clearly demonstrate that the mode of entry into the proteasome has a strong effect on the repertoire of epitopes that are presented, as predicted above.

Calculations of the force needed to unfold the C and N termini predict the direction of translocation.

These data strongly suggest that the presence of a loosely folded C or N terminus on a polypeptide determines whether the proteasome degrades the polypeptide starting from that end. We therefore reasoned that calculation of the force needed to unfold the N or C terminus of a given protein may predict the direction of proteasomal degradation. We generated computer simulations (based on a GO like algorithm), in which a given protein with a known structure is "pulled" from either its N- or C-terminus. “Virtual springs” were connected to both ends of the protein and one of the termini was pulled with a constant velocity and the magnitude of the force applied on the virtual moving spring, as the terminus is unraveled is calculated. In these simulations, the pulling force was acting against internal forces in the molecule (enthalpy) and was gradually increased to overcome the resisting forces.

Snapshots, of the unfolding of MBP during the pulling simulations using low constant velocity illustrate the sequence that was released from each end along the simulation, are shown in Figure 7A & S7. An unfolded C-terminus was obtained at the early stages of the pulling and its length gradually increased. Only, when the C-terminal tail reached 40 residues, the N-terminal tail began to protrude from the globular protein, indicating that unfolding the C-terminal was more easily achieved. These observations indicate that the C-terminus of MBP is more susceptible to mechanical unfolding than its N-terminus and may account for its C to N degradation by the proteasome.

When a similar simulation was applied to native ovalbumin, the opposite outcome was obtained (Figures 7B & S7). These results predict N to C degradation, which is consistent with the directionality of ovalbumin’s degradation by proteasomes *in vivo.* Naturally, this energetic analysis should not apply to the degradation of denatured (molten globule) ovalbumin by purified proteasomes.

The calculated magnitude of force required to unfold calmodulin was 2-3 fold smaller than that measured for MBP and ovalbumin and comparable when pulling from either the N- or the C-terminus (Figure 7C), which can account for calmodulin’s degradation in either direction. Although calmodulin has a rather symmetric structure, the forces needed for the unwinding of its N and C-termini were not identical, and the C-terminus was unfolded somewhat more easily (Figures S7). Perhaps accounting, for the intermediate degradation products seen upon proteolysis from N but not the C-terminus (compare calmodulin-RFP to RFP-calmodulin in Figure 1E). Together, these *in silico* analyses suggest that if the local tendency of protein termini to unravel is significantly different, proteasomal degradation tend to begin at the less stable terminus.

DISCUSSION

The present findings argue strongly that the initiation site for translocation is determined primarily by the presence of a loosely folded terminus or its tendency to be unraveled, rather than by the location of the ubiquitin tag. While the location of the ubiquitin tag on the target protein may perhaps influence directional preference (Prakash et al., 2004), it seems most likely that ATP-driven conformational changes or exposure of hydrophobic surfaces on the ATPase (Medalia et al., 2009) promote local unfolding and tight binding of the substrate's less stable terminus, which then becomes the initiation site for translocation. Because the directionality seen with the archaeal PAN complex resembled that of the 26S proteasomes for several substrates, it seems most likely that the hexameric ATPases at the base of the 19S particle are both necessary and sufficient to bind and unfold the terminus of the protein. Accordingly, no directional preference was found for 20S proteasomes (Figure 1).

Calculations comparing the forces necessary to unwind the C- and N-termini suggest that the inherent thermodynamic stabilities of the terminal regions determine the directionality of degradation (Figure 7). Thus, translocation appears to be initiated at the terminus that is either inherently unfolded (as in denatured ovalbumin, casein or p21) or is easier to unwind as in the globular proteins MBP and native ovalbumin. Although similar studies with many proteins will be important to establish the generality of these results, these findings imply that the direction of translocation of a protein can be predicted based only on its crystal structure and energetic calculations of the forces necessary to unwind its ends.

Initiating translocation from an internal vs terminal unstructured domain

Although the present findings with substrates bearing a blocked terminus can be best explained by translocation from a loosely folded terminus, the initiation of degradation from an internal unstructured domain is clearly important. Such a mechanism is of special interest in those instances where proteasomal degradation is incomplete and releases an active domain that functions in cell regulation. The best studied such example is the 50k subunit of the transcription factor NFκB which is generated by 26S proteasomes from a 105kDa precursor, especially in inflammatory states. Similarly the active forms of the yeast transcription factors SPT23 and MGA2 are generated by proteasomal hydrolysis of internal loose domains that anchor the large precursors to the ER membrane (Hoppe et al., 2000).

Exactly why the tightly folded RFP domains were unfolded and digested when only one of the termini was blocked and not with GFP-p21-CFP and RFP-Ova-RFP or with the SPT23, MGA2 and NFκB precursors is an important issue for future investigation. Furthermore, because this directional degradation of substrates with a single blocked terminus had distinct consequences than proteolysis initiated from an internal loop (i.e. only the former led to processive degradation of GFP/CFP/RFP domains or allowed generation of the SIINFEKL epitope *in vivo*), these two modes of degradation must involve distinct mechanisms. Similarly, unidirectional proteolysis (calmodulin & p21) cannot be due to proteasomes in both cases (N or C-terminally blocked) simply beginning at an internal loop within the loosely folded polypeptide chain.

The direction of translocation influence on the spectrum of peptides produced and thus MHC class I antigen presentation

The mirror-image symmetry of the two β-rings at the center of the 20S complex (Groll et al., 1997; Lowe et al., 1995b) implies that an unfolded polypeptide translocated from its N terminus should interact with the active sites of one β-ring with the same stereochemistry and in the same manner as that polypeptide would interact with the other ring if translocated from its C terminus. Therefore, no additional entropic penalty should discriminate between translocation from either end, since theoretically a polypeptide entering the central chamber in an extended configuration does not need to change its orientation within the particle in order to assume a preferred position for binding to any of the active sites. Furthermore, recent NMR studies of the 20S suggest that the outer chamber formed between the α-and β-subunits favors the maintenance of an unstructured conformation of the polypeptide (Ruschak et al., 2010).

Therefore, it was a surprise to find that the direction of translocation of p21 and denatured ovalbumin influenced markedly the profile of proteasomal degradation products, as corroborated by two complementary approaches: MS and quantitative size distribution. It is noteworthy that degradation of p21 in an N to C direction was significantly faster and yielded a much greater diversity of products than in the C to N direction, perhaps the flux of translocation affects the handling of the substrate within the 20S chamber.

The peptides generated only upon translocation from either direction were derived from all parts of the protein sequence, therefore, product generation is truly dependent upon the direction of substrate translocation and is not an artifact of the experimental design (e.g. as might have occurred if the diversity of products was restricted to the terminus tethered by the non-translocatable moiety and therefore less able to diffuse freely within the central chamber). It is also important to note that even when a substrate enters in a given direction, specific sequences are cut in a multitude of different fashions leading to the release of a variety of different overlapping products. Furthermore, when degradation occurred in the two opposite directions, a variety of overlapping but distinct peptides were produced from the same region of the protein. This clustering of unique peptide products implies that the 20S's active sites begin to cleave at quite different residues when a substrate enters in the opposite direction. Although the proteasome's outer chamber has hydrophobic patches that can interact with the polypeptide in transit (Ruschak et al., 2010) and reduce its tendency to refold. Yet, the polypeptide or its cleaved longer fragments may subsequently assume secondary structures within the central chamber that affect their further cleavage susceptibility. The effects of directionality found here suggest that the degree of secondary structure of the polypeptide as it reaches the proteasome's six active sites and how the upstream or downstream neighboring sequences bind to the active sites will determine if any specific sequence is cleaved.

The present studies demonstrate a large difference in the efficiency of presentation of the immunodominant ovalbumin epitope, when this protein was digested from its N-terminus or from an internal loop. The dramatic difference in presentation of this well-studied epitope presumably is due to the major differences in the spectrum of peptides generated from ovalbumin and predicts a similar large influence of directionality on the yields of epitopes in other proteins. Further tests of this prediction will be important to undertake and has not been considered in the immunology literature. There have been numerous *in vitro* studies that have followed the production by isolated 20S proteasomes and immunoproteasomes of specific epitopes from longer oligopeptide precursors. The present findings argue strongly that the use of small peptide substrates in such experiments will often not reflect the actual pattern of product generation by 26S proteasomes when the antigenic protein is delivered to the active sites in a specific direction in an ATP-dependent manner.

The efficiency of presentation of a specific epitope on surface MHC Class I molecules depends largely on the rate of breakdown of the protein as well as the frequency of generation of the epitope during proteasomal degradation (Kohler et al., 2001; Rock et al., 2004). It has long been recognized that many sequences in proteins that have the potential of binding to MHC Class I molecules are not presented and are not immunodominant, because they fail to be released by the proteasome (e.g. if the proteasome's or immunoproteasome's active sites cleave within and destroy the potential epitope). The present findings demonstrate that not only the location of the epitope within the polypeptide and its flanking sequences but also the direction of polypeptide translocation into the 20S by the 19S ATPases have a large influence on the immunogenicity of proteins.

Materials and Methods

Generation of proteasome substrates

Substrates used in this study were purified using on Ni-NTA standard affinity purification procedures. Detailed descriptions are presented in supplementary materials and methods.

Degradation assays with pure proteasomes

PAN and archaeal 20S proteasomes were purified, as described elsewhere (Navon and Goldberg, 2001). Mammalians 20S and 26S proteasome were purified from rabbit muscles as described previously (Kisselev et al., 1999). Detailed descriptions of the degradation reactions and there analysis are presented in supplementary materials and methods.

Mass spectrometry analysis

Approximately 5µg of protein were incubated with ~10nM of rabbit 26S proteasomes in buffer containing 50mM Hepes, pH 7.5, 5mM $MgCl_2$, 1mM DTT and 2mM ATP or rabbit 20S proteasomes in buffer containing 50mM Hepes pH 7.5, 5mM $MgCl_2$ and 1 mM DTT in the presence or absence of 0.02% SDS at 37ºC for 5 hours. Following the reaction, samples were ultrafiltrated through 10kDa cutoff and the products were subjected to mass spectrometry analysis by LC-MS/MS on LTQ-Orbitrap (Thermo-Fisher). Peptides were identified by Mascot and Sequest software against the sequences of ovalbumin (residues 52-412) and p21. Detailed description of the quantitative comparison of proteasomal degradation products and their quantitative size distribution determination are provided in the supplementary materials and methods.

Generation of EL4 cells expressing p21 and ovalbumin variants fused to RFP

Ovalbumin and p21 fused to RFP were cloned into pMIG, a retroviral expression vector, which harbors an IRES-GFP element. Viruses were generated in 293T cells by triple transfection with Env and Gag-pol encoding vectors as described (Drori et al, Mol. Immunol 2010). Transduced EL4 cells (mouse thymoma cells) were sorted for GFP-positive to 100% purity by FACS (Aria, BD), and cultured in RPMI 1640 medium supplemented with 10% fetal bovine serum, 2mM glutamine, 50 units/ml Penicillin, 50µg/ml Streptomycin, 1x nonessential amino acids and 1 mM sodium pyruvate.

Measurement of protein stability in cells

EL4 cells transduced with ovalbumin and p21 derivatives were pre-incubated for 1 hour at 37 °C in the presence and in the absence of 2µM bortezomib. Cycloheximide (50µg/ml) was then added to the medium, and cells were incubated at 37ºC for up to 6 hours. Equal numbers of cells were withdrawn at the indicated time points, washed with Phosphate-buffered saline and lysed with 200µl of NP-40 lysis buffer (1% NP-40, 150 mM NaCl, 0.5%sodium-deoxycholate, 0.1% SDS, 1mM EDTA, 1mM EGTA, 0.1mM leupeptin, 0.5mM pepstatin, 2 µg/ml aprotinin, 1mM PMSF in 25mM Tris, pH 7.5). The mixture was incubated on ice for 15 minutes and centrifuged at 16,000X*g* for 10 min at 4°C. Supernatants were then subjected to immunobloting with the indicated antibodies. The immunoblots were quantified by densitometry (Quantity One, Bio-Rad).

Monitoring the levels of H-2K^b/ SIINFEKL complex on EL4 Cells surface

About 10^6 EL4 cells of interest were washed with FACS washing buffer (PBS, 0.5% BSA, 0.1% NaN_3) and incubated for 60 min on ice with 25D1.16, a mouse monoclonal antibody (kindly provided by Dr. Ron Germain, National Institutes of Health), which recognizes the H-2K^b/ SIINFEKL complex. Cells were then washed three times with the buffer and incubated on ice with Alexa Fluor 647-conjugated anti mouse polyclonal antibody for 60 min (Molecular Probes). Consequently, the cells were resuspended in PBS and analyzed by FACS (BD Biosciences). Mean fluorescence intensity (MFI) was calculated using FACSdiva software (BD Biosciences).

In silico **calculation of termini availability of the different substrate**

The *in silico* calculation procedure is described in the supplementary materials and methods.

References

Beskow, A., Grimberg, K.B., Bott, L.C., Salomons, F.A., Dantuma, N.P., and Young, P. (2009). A conserved unfoldase activity for the p97 AAA-ATPase in proteasomal degradation. J Mol Biol *394*, 732-746.
Cascio, P., Call, M., Petre, B.M., Walz, T., and Goldberg, A.L. (2002). Properties of the hybrid form of the 26S proteasome containing both 19S and PA28 complexes. EMBO J *21*, 2636-2645.
Cascio, P., Hilton, C., Kisselev, A.F., Rock, K.L., and Goldberg, A.L. (2001). 26S proteasomes and immunoproteasomes produce mainly N-extended versions of an antigenic peptide. EMBO J *20*, 2357-2366.
Chen, X., Chi, Y., Bloecher, A., Aebersold, R., Clurman, B.E., and Roberts, J.M. (2004). N-acetylation and ubiquitin-independent proteasomal degradation of p21(Cip1). Mol Cell *16*, 839-847.
Groll, M., Bajorek, M., Kohler, A., Moroder, L., Rubin, D.M., Huber, R., Glickman, M.H., and Finley, D. (2000). A gated channel into the proteasome core particle. Nat Struct Biol *7*, 1062-1067.
Groll, M., Ditzel, L., Lowe, J., Stock, D., Bochtler, M., Bartunik, H.D., and Huber, R. (1997). Structure of 20S proteasome from yeast at 2.4 A resolution. Nature *386*, 463-471.
Hagai, T., and Levy, Y. (2010). Ubiquitin not only serves as a tag but also assists degradation by inducing protein unfolding. Proc Natl Acad Sci U S A *107*, 2001-2006.
Hoppe, T., Matuschewski, K., Rape, M., Schlenker, S., Ulrich, H.D., and Jentsch, S. (2000). Activation of a membrane-bound transcription factor by regulated ubiquitin/proteasome-dependent processing. Cell *102*, 577-586.
Howarth, M., Williams, A., Tolstrup, A.B., and Elliott, T. (2004). Tapasin enhances MHC class I peptide presentation according to peptide half-life. Proceedings of the National Academy of Sciences of the United States of America *101*, 11737-11742.
Humphrey, W., Dalke, A., and Schulten, K. (1996). VMD: visual molecular dynamics. J Mol Graph *14*, 33-38, 27-38.
Kisselev, A.F., Akopian, T.N., and Goldberg, A.L. (1998). Range of sizes of peptide products generated during degradation of different proteins by archaeal proteasomes. J Biol Chem *273*, 1982-1989.
Kisselev, A.F., Akopian, T.N., Woo, K.M., and Goldberg, A.L. (1999). The sizes of peptides generated from protein by mammalian 26 and 20 S proteasomes. Implications for understanding the degradative mechanism and antigen presentation. J Biol Chem *274*, 3363-3371.
Kohler, A., Cascio, P., Leggett, D.S., Woo, K.M., Goldberg, A.L., and Finley, D. (2001). The axial channel of the proteasome core particle is gated by the Rpt2 ATPase and controls both substrate entry and product release. Mol Cell *7*, 1143-1152.
Kuboniwa, H., Tjandra, N., Grzesiek, S., Ren, H., Klee, C.B., and Bax, A. (1995). Solution structure of calcium-free calmodulin. Nat Struct Biol *2*, 768-776.
Liu, C.W., Corboy, M.J., DeMartino, G.N., and Thomas, P.J. (2003). Endoproteolytic activity of the proteasome. Science *299*, 408-411.
Lowe, J., Stock, D., Jap, B., Zwickl, P., Baumeister, W., and Huber, R. (1995a). Crystal structure of the 20S proteasome from the archaeon T. acidophilum at 3.4 A resolution. Science *268*, 533-539.
Lowe, J., Stock, D., Jap, B., Zwickl, P., Baumeister, W., and Huber, R. (1995b). Crystal structure of the 20S proteasome from the archaeon T. acidophilum at 3.4 A resolution [see comments]. Science *268*, 533-539.

Medalia, N., Beer, A., Zwickl, P., Mihalache, O., Beck, M., Medalia, O., and Navon, A. (2009). Architecture and molecular mechanism of PAN, the archaeal proteasome regulatory ATPase. J Biol Chem *284*, 22952-22960.
Navon, A., and Goldberg, A.L. (2001). Proteins are unfolded on the surface of the ATPase ring before transport into the proteasome. Mol Cell *8*, 1339-1349.
Peth, A., Uchiki, T., and Goldberg, A.L. (2010). ATP-Dependent Steps in the Binding of Ubiquitin Conjugates to the 26S Proteasome that Commit to Degradation. Mol Cell *40*, 671-681.
Porgador, A., Yewdell, J.W., Deng, Y., Bennink, J.R., and Germain, R.N. (1997). Localization, quantitation, and in situ detection of specific peptide-MHC class I complexes using a monoclonal antibody. Immunity *6*, 715-726.
Prakash, S., Tian, L., Ratliff, K.S., Lehotzky, R.E., and Matouschek, A. (2004). An unstructured initiation site is required for efficient proteasome-mediated degradation. Nat Struct Mol Biol *11*, 830-837.
Rabl, J., Smith, D.M., Yu, Y., Chang, S.C., Goldberg, A.L., and Cheng, Y. (2008). Mechanism of gate opening in the 20S proteasome by the proteasomal ATPases. Mol Cell *30*, 360-368.
Rock, K.L., and Goldberg, A.L. (1999). Degradation of cell proteins and the generation of MHC class I-presented peptides. Annu Rev Immunol *17*, 739-779.
Rock, K.L., York, I.A., and Goldberg, A.L. (2004). Post-proteasomal antigen processing for major histocompatibility complex class I presentation. Nat Immunol *5*, 670-677.
Rock, K.L., York, I.A., Saric, T., and Goldberg, A.L. (2002). Protein degradation and the generation of MHC class I-presented peptides. Adv Immunol *80*, 1-70.
Ruschak, A.M., Religa, T.L., Breuer, S., Witt, S., and Kay, L.E. (2010). The proteasome antechamber maintains substrates in an unfolded state. Nature *467*, 868-871.
Shabek, N., Herman-Bachinsky, Y., and Ciechanover, A. (2009). Ubiquitin degradation with its substrate, or as a monomer in a ubiquitination-independent mode, provides clues to proteasome regulation. Proc Natl Acad Sci U S A *106*, 11907-11912.
Shen, L., and Rock, K.L. (2004). Cellular protein is the source of cross-priming antigen in vivo. Proc Natl Acad Sci U S A *101*, 3035-3040.
Smith, D.M., Kafri, G., Cheng, Y., Ng, D., Walz, T., and Goldberg, A.L. (2005). ATP binding to PAN or the 26S ATPases causes association with the 20S proteasome, gate opening, and translocation of unfolded proteins. Mol Cell *20*, 687-698.
Swaisgood, H.E. (2003). Chemistry of the caseins. Advanced Dairy Chemistry-1 Proteins *Part A.*, 139–202.
Takeuchi, J., Chen, H., and Coffino, P. (2007). Proteasome substrate degradation requires association plus extended peptide. EMBO J *26*, 123-131.
Tani, F., Shirai, N., Onishi, T., Venelle, F., Yasumoto, K., and Doi, E. (1997). Temperature control for kinetic refolding of heat-denatured ovalbumin. Protein Sci *6*, 1491-1502.
Whitby, F.G., Masters, E.I., Kramer, L., Knowlton, J.R., Yao, Y., Wang, C.C., and Hill, C.P. (2000). Structural basis for the activation of 20S proteasomes by 11S regulators. Nature *408*, 115-120.

ACKNOWLEDGMENTS

A.N is an incumbent of the Recanati career development chair of cancer research. Research in the laboratory of A.N. is supported by the Israel Science Foundation (ISF), the Minerva Foundation (Germany), the German-Israeli Foundation for Scientific Research and Development (GIF), and a special gift from Rolando Uziel. These studies were also supported in part by a grant to ALG from the NIH (GM05 1923-10)

Figure Legends

Figure 1: Certain proteins are exclusively degraded from their N or C termini, while others can be degraded from either end.

(A) MBP is translocated into the proteasome exclusively from its C terminus. MBP cross-linked to agarose beads through its C (MBP-agarose) or N-terminus (agarose-MBP) was incubated with PAN and 20S proteasomes for the indicated time. The beads were washed three times and boiled with SDS sample buffer. **(B) β-casein is degraded exclusively from its N-terminus**. Time course of degradation of β-Casein cross-linked to agarose beads through its C (Casein-agarose) or N-terminus (agarose-Casein). Reactions were performed and analyzed as is described in A. **(C)** Time course of degradation of β-casein linked to biotin or avidin (attached to the biotin) on its N or C terminus by 26S proteasomes. **(D)** β-casein is degraded from both termini by the SDS-activated mammalian 20S proteasome. β-casein linked to avidin through its C (Casein-avidin) or N terminus (avidin-Casein) was incubated with SDS activated purified rabbit 20S proteasomes. Equal portions were removed and subjected to Western blot analysis using anti-His antibodies. **(E)** Blocking either terminus of Apo-calmodulin does not prevent its proteasomal degradation. Time course of calmodulin-RFP and RFP-calmodulin degradation by PAN-20S complex. Aliquots of the reaction mixture were removed at the indicated times and analyzed by Western blot using anti-RFP antibody.

Figure 2: p21 and denatured (molten-globule) ovalbumin are degraded by mammalian 20S and 26S proteasomes with either terminus blocked. Time course of p21 N or C terminally fused to RFP degradation by mammalian 20S proteasome **(A)** or 26S proteasome **(B)**. **(C)** Large excess of p21-RFP & RFP-21 (3µM) were incubated with 26S proteasome (1nM), a portion (1:5) of the initial material and following one hour of incubation was blotted with anti RFP. **(D)** Time course of ova-RFP and RFP-ova

degradation by mammalian 26S proteasomes. Right: Quantification of the residual amount of protein at each time point, are presented (SD were calculated from four repetitions under similar conditions).

Figure 3: Directionality of proteasomal degradation in living cells. EL4 cells expressing p21 or ovalbumin N or C-terminally fused to RFP were pre-incubated at 37°C in the presence and absence of 2µM bortezomib (Velcade). After 1 hour cycloheximide was added (50 µg/ml) to the medium for the indicated times. Thereafter, equal numbers of cells were lysed, and the supernatants were subjected to Western blot analyses by anti-RFP and anti-actin antibodies. **(A)** Cycloheximide chase of EL4 cells expressing p21 fused to RFP either through its C or N-terminus. (**B**) Cycloheximide chase of EL4 cells expressing ovalbumin fused to RFP either through its C or N-terminus. Quantification of the residual amount of protein detected at each time point during the chycloheximide chase are presented (SD were calculated from three repetitions under similar conditions).

Figure 4: Blocking both of p21 termini lead to internal Initiation of its proteasomal degradation and sparing of the up-and downstream neighboring globular domains, *in vitro* and *in vivo*.

(A) Right panel: To capture all of the proteasomal degradation products and intermediates (*in vitro*) large excess of His-GFP-p21-CFP-Flag (3µM) was incubated with 26S proteasome (1nM). A portion (1:5) of the initial material, and following one hour of incubation were blotted with anti GFP. **Left panel:** Time course of *in vitro* degradation of GFP-p21-CFP showing the accumulation of the GFP (anti His) and CFP (anti Flag) domains upon hydrolysis of the full length GFP-p21-CFP. **(B) Left panel:** Western blot analysis of total cell lysat prepared for EL4 cells expressing His-GFP-p21-CFP-Flag in the presence and absence of Velcade. The large ratio in favor of the intact GFP and CFP domains to the full-length (more than hundred fold) demonstrate the stability and the quantitative release of these domains in the *in vivo* proteasomal degradation of GFP-p21-CFP. **Right panel:** Time course of *in vivo* degradation of GFP-p21-CFP showing the accumulation of the GFP (anti His) and CFP (anti Flag) domains upon hydrolysis of the full length GFP-p21-CFP. **(C)** Time course of *in vivo* degradation of p21-RFP & RFP-p21 (as in Figure 2A) demonstrating the processive degradation of the RFP domain upon *in vivo* proteasomal degradation of p21 blocked on either termini by RFP.

Figure 5: (A) The 26S proteasome generated different spectrum of peptides from p21 upon degradation from its N or C-terminus and much greater diversity in the N to C direction. Following digestion of RFP-p21 and p21-RFP by 26S proteasomes, equal amounts of the degradation products (as estimated by fluorescamine) were analyzed by MS. Prior to the analysis one set of peptides was labeled by reductive dimethylation with deuterium-and ^{13}C, 'heavy', formaldehyde and the other set treated with non-isotopic formaldehyde. The samples were mixed, and the isotopic ratios in the individual peptides were analyzed by mass spectrometry. These experiments were repeated three times with standard deviations of less than 10%. The raw data of both analyses is presented in Figure S4. **(B) Size distribution of peptides generated from p21-RFP and RFP-p21.** Peptides generated during degradation of p21-RFP and RFP-p21 by 20S (without SDS activation) and 26S proteasomes were separated from undigested protein by ultrafiltration through a 10kDa cutoff membrane. Equal amounts of peptide products were reacted with fluorescamine and immediately fractionated on a high-performance size exclusion column. The fluorescence of eluted material was monitored continuously with a fluorescence detector and a blank run (corresponding to time 0) was always subtracted. Molecular weights were calculated from the calibration curve shown in Figure S6. Similar data were obtained in at least four independent experiments.

Figure 6: SIINFEKL is presented on surface H2-K^b molecules of EL4 cells expressing ova-RFP but much less in cells expressing RFP-ova-RFP. (A) Western blot analysis of total cell lysate prepared from EL4 cells expressing HA-RFP-ova-RFP-His in the presence and absence of Velcade. The much greater content (more than a hundred fold) of the intact RFP domains compared to the full-length substrates demonstrates that RFP is quantitatively released and not degraded during the *in vivo* proteasomal degradation of RFP-ova-RFP. Both the N-terminal and the C-terminal RFP domains were spared, as is evident from the immunoreactivity of the RFP domains with HA and His antibodies. **(B)** EL4 cells expressing ova-RFP (blue), RFP-ova-RFP (black) or empty vector (red), were stained with 25D1.16 monoclonal antibody, recognizing the H2-K^b/SIINFEKL complex. For detection, Alexa Fluor 647-conjugated anti-mouse was used as a secondary antibody. Live cells were gated based on their light scatter characteristics. To ensure similar levels of expression, a narrow GFP (pMIG vector internal iris) gate was selected.

Figure 7: *In silico* calculation of the force needed to unravel the N or the C terminus of MBP, apo-calmodulin and ovalbumin. The graphs on the left depict the length of the unstructured tail that was predicated to form (along the simulation) upon pulling the molecule either from its N' (black) or C' (red) terminus. The "snapshots" (generated with VMD (Humphrey et al., 1996)) on the right are representative structures of the proteins along the simulations at the time steps specified at the graphs.

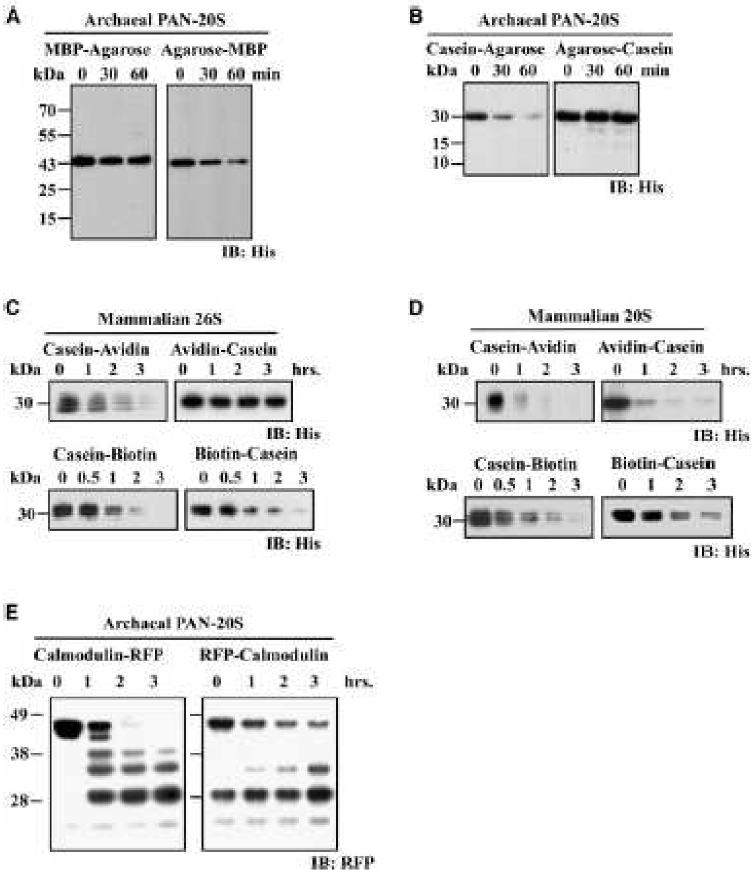
A
Archaeal PAN-20S
MBP-Agarose
Agarose-MBP
kDa 0 30 60
0 30 60 min
70
55
43
25
15
IB: His
B
Archaeal PAN-20S
Casein-Agarose
Agarose-Casein
kDa 0 30 60
0 30 60 min
30
15
10
IB: His
C
Mammalian 26S
Casein-Avidin
Avidin-Casein
kDa 0 1 2 3
0 1 2 3 hrs.
30
IB: His
Casein-Biotin
Biotin-Casein
kDa 0 0.5 1 2 3
0 0.5 1 2 3
30
IB: His
D
Mammalian 20S
Casein-Avidin
Avidin-Casein
kDa 0 1 2 3
0 1 2 3 hrs.
30
IB: His
Casein-Biotin
Biotin-Casein
kDa 0 0.5 1 2 3
0 1 2 3
30
IB: His
E
Archaeal PAN-20S
Calmodulin-RFP
RFP-Calmodulin
kDa 0 1 2 3
0 1 2 3 hrs.
49
38
28
IB: RFP

Figure 1

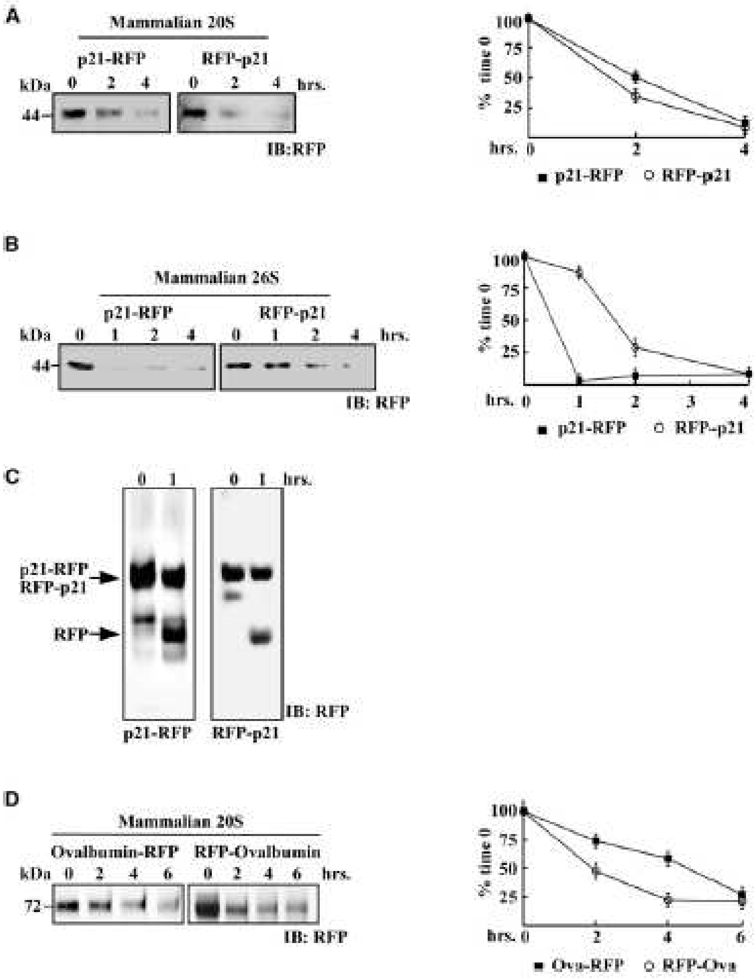

A
Mammalian 20S
p21-RFP
RFP-p21
kDa 0 2 4 0 2 4 hrs.
44
IB:RFP
100
75
50
25
% time 0
hrs. 0 2 4
p21-RFP
RFP-p21
B
Mammalian 26S
p21-RFP
RFP-p21
kDa 0 1 2 4 0 1 2 4 hrs.
44
IB: RFP
100
75
50
25
% time 0
hrs. 0 1 2 3 4
p21-RFP
RFP-p21
C
0 1 0 1 hrs.
p21-RFP
RFP-p21
RFP
IB: RFP
p21-RFP
RFP-p21
D
Mammalian 20S
Ovalbumin-RFP
RFP-Ovalbumin
kDa 0 2 4 6 0 2 4 6 hrs.
72
IB: RFP
100
75
50
25
% time 0
hrs. 0 2 4 6
Ova-RFP
RFP-Ova

Figure 2

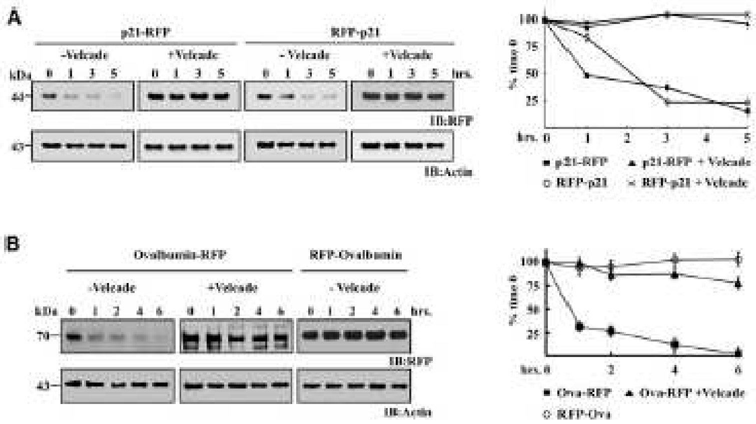
A
p21-RFP
RFP-p21
-Velcade
+Velcade
- Velcade
+Velcade
kDa
0 1 3 5
hrs.
44
IB:RFP
43
IB:Actin
% time 0
100
75
50
25
hrs. 0 1 2 3 4 5
p21-RFP
p21-RFP + Velcade
RFP-p21
RFP-p21 + Velcade
B
Ovalbumin-RFP
RFP-Ovalbumin
-Velcade
+Velcade
- Velcade
kDa
0 1 2 4 6
hrs.
70
IB:RFP
43
IB:Actin
% time 0
100
75
50
25
hrs. 0 2 4 6
Ova-RFP
Ova-RFP +Velcade
RFP-Ova

Figure 3

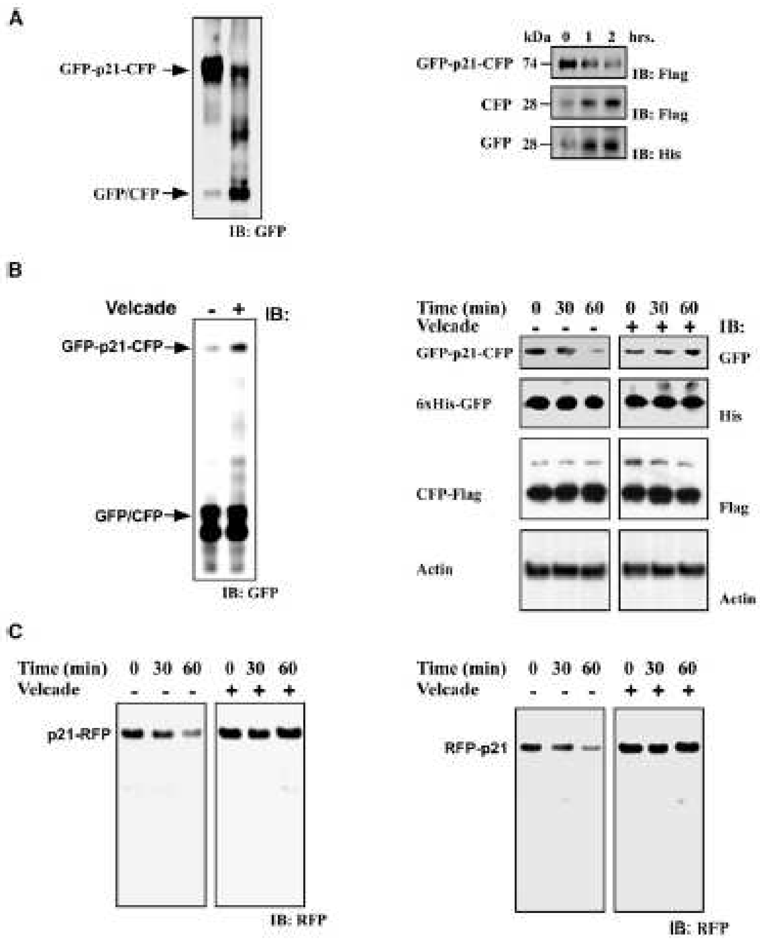
A
GFP-p21-CFP
GFP/CFP
IB: GFP
kDa 0 1 2 hrs.
GFP-p21-CFP 74
IB: Flag
CFP 28
IB: Flag
GFP 28
IB: His
B
Velcade - +
IB:
GFP-p21-CFP
GFP/CFP
IB: GFP
Time (min) 0 30 60 0 30 60
Velcade - - - + + +
IB:
GFP-p21-CFP
GFP
6xHis-GFP
His
CFP-Flag
Flag
Actin
Actin
C
Time (min) 0 30 60 0 30 60
Velcade - - - + + +
p21-RFP
IB: RFP
Time (min) 0 30 60 0 30 60
Velcade - - - + + +
RFP-p21
IB: RFP

Figure 4

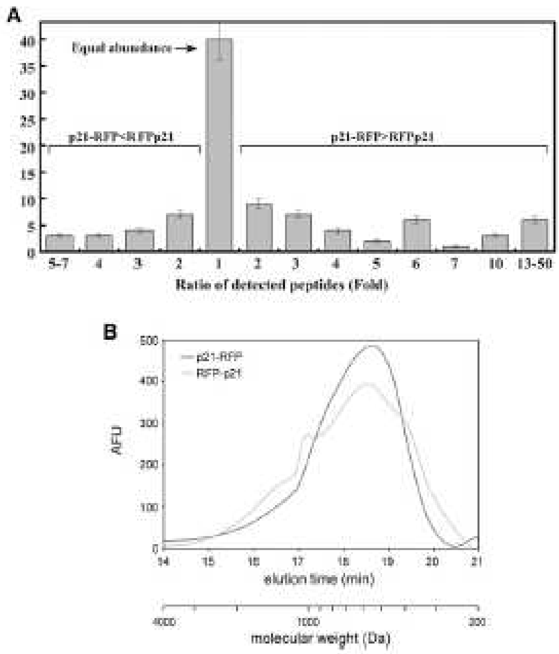

Figure 5

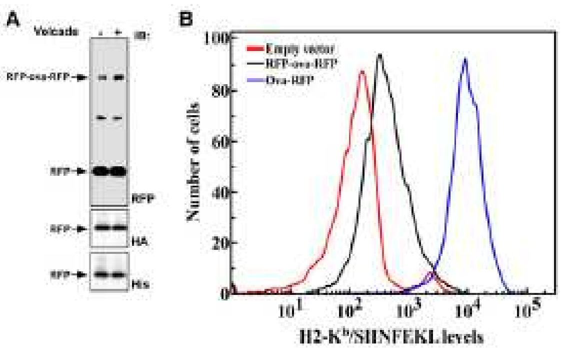

Figure 6

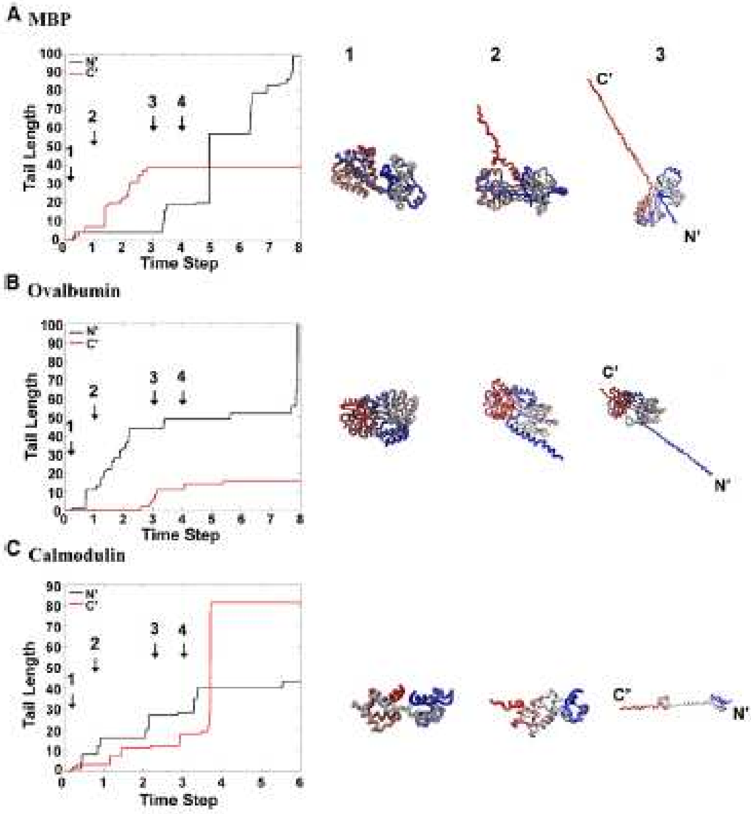

Figure 7